Coordination dependence of hyperfine fields of 5sp impurities on Ni surfaces

2003 J. Phys.: Condens. Matter 15 8115

(http://iopscience.iop.org/0953-8984/15/47/014)

INSTITUTE OF PHYSICS PUBLISHING JOURNAL OF PHYSICS: CONDENSED MATTER

J. Phys.: Condens. Matter **15** (2003) 8115–8122 PII: S0953-8984(03)69665-7

Coordination dependence of hyperfine fields of 5sp impurities on Ni surfaces

Phivos Mavropoulos

Institut für Festkörperforschung, Forschungszentrum Jülich, D-52425 Jülich, Germany

E-mail: Ph.Mavropoulos@fz-juelich.de

Received 26 September 2003
Published 14 November 2003
Online at stacks.iop.org/JPhysCM/15/8115

Abstract

We present first-principles calculations of the magnetic hyperfine fields H_{hf} of 5sp impurities on the (001), (111), and (110) surfaces of Ni. We examine the dependence of H_{hf} on the coordination number by placing the impurity in the surfaces, on top of them at the adatom positions, and in the bulk. We find a strong coordination dependence of H_{hf}, different and characteristic for each impurity. The behaviour is explained in terms of the on-site s–p hybridization as the symmetry is reduced at the surface. Our results are in agreement with recent experimental findings.

1. Introduction

The understanding of the magnetic properties of solids on the atomic level is a challenge for experiment and theory. The magnetic hyperfine interaction of the electronic magnetization with the nuclear magnetic moment of an atom is such a property, and it is known to depend in turn on the properties of the atom as well as on the neighbouring atomic environment. In particular, for impurities in the bulk of the ferromagnetic materials Fe, Co, Ni, the trends of magnetic hyperfine field H_{hf} have been well understood, and the experimental and theoretical results extend over practically the whole periodic table [1, 2]. The relation of H_{hf} to the local magnetic moment and to the atomic environment is not trivial. Therefore, for the interpretation of the trends, first-principles, all-electron methods have been extremely useful [2], since they can describe the charge density and magnetization near the atomic nucleus self-consistently. H_{hf} measurements for probe atoms at interfaces or surfaces can also provide unique information on the local structure [3], especially in combination with relevant calculations [4–6].

One of the modern powerful experimental techniques allowing the study of the hyperfine interaction of impurities at surfaces or interfaces is perturbed angular correlation spectroscopy [7]. It has a high enough sensitivity to allow accurate measurements from highly

0953-8984/03/478115+08$30.00

Table 1. Impurity positions on Ni surfaces and in bulk and their coordination numbers N. S: the impurity is in the surface layer; $S+1$: the impurity is on top of the layer in the hollow adatom position; $S-1$: the impurity is in the sub-surface layer; (111) kink: the impurity is on top of a (111) surface at a kink.

Surface position	(111) $S+1$	(001) $S+1$	(110) $S+1$	(111) Kink	(110) S	(001) S	(111) S	(110) $S-1$	Bulk
N	3	4	5	6	7	8	9	11	12

diluted probe atoms (10^{-4}–10^{-5} of a monolayer), so these form practically isolated impurities. In a recent experimental publication [8], the coordination number dependence of $H_{\rm hf}$ for Cd impurities in a Ni host was studied, by comparing data from Cd positioned on several Ni surfaces. The conclusion was that the $H_{\rm hf}$ for Cd strongly depends on the coordination number. Although this might be expected, since the magnetic moment of the Cd impurity is not intrinsic but rather induced by the environment, the data show neither a linear dependence nor an increase with the number N of Ni neighbours. On the contrary, $H_{\rm hf}$ is measured to be strongest for $N = 3$, while as N is progressively increased $H_{\rm hf}$ seems to change sign and has a parabolic behaviour.

Although calculations for sp impurities on Ni surfaces exist [6, 9], they concern only 4sp impurities on Ni(001), so no clear conclusion on the trends of $H_{\rm hf}$ with respect the coordination number can be drawn. Here, in order to interpret the experimental findings, we have performed first-principles calculations for all 5sp and the early 6s impurities (Ag–Ba) on top of the Ni(001), (111), and (110) surfaces, within the surface layers, and in bulk Ni in a substitutional position. The impurity positions studied are given in table 1 together with the coordination numbers. In this way we obtain systematic trends of $H_{\rm hf}$ related both to the coordination number and to the impurity atomic number. In all cases the impurities were assumed to be on the ideal lattice positions with the experimental fcc Ni lattice constant; relaxations were not accounted for.

2. Method of calculation

The calculations are based on the local spin density approximation of density-functional theory. The full-potential Korringa–Kohn–Rostoker Green function method for defects in bulk or at surfaces is employed [10], with an exact description of the atomic cells [11]. In short, after calculating the electronic structure of the host medium (bulk or surface) self-consistently, we use the Green function of this reference system to calculate the electronic structure of the distorted system containing the impurity via an algebraic Dyson equation. The power of the method lies in it working in real space with the boundary condition of the infinite host included, rather than in k-space with a supercell construction. The Green function $G^{nn'}_{lm;l'm'}(E)$ is described in cell-centred coordinates around cells n and n', and expanded in cell-centred solutions of the Schrödinger equation with angular momenta (l, m) and (l', m'). The impurity and a cluster containing the 12 first neighbours is perturbed in our calculations; this is enough because the fcc crystal structure is close packed. Increasing the cluster to contain the second neighbours in a test case caused insignificant changes in our results. A truncation of the angular momentum to $l_{\rm max} = 3$ was imposed. In a final step, the trace of the Green function is used to obtain the (l, m) decomposed charge density and magnetic moment. We use the scalar relativistic approximation [12], which takes into account the relativistic effects other than the spin–orbit interaction and retains spin as a good quantum number.

3. Discussion

In the case of spin magnetism, the dominant contribution to $H_{\rm hf}$ is the Fermi contact interaction relating it directly to the spin density at the nucleus, $m(\mathbf{r}=0)$. In a non-relativistic treatment this has the simple form

$$H_{\rm hf} = \frac{8\pi}{3} m(\mathbf{r}=0). \tag{1}$$

In a scalar relativistic treatment, as in the present paper, Breit's formula has to be used instead to average $m(\mathbf{r})$ over the Thomson radius of the nucleus [2, 13]. In any case the magnetization at or near the nuclear position is important, and determined by the s wavefunctions alone, since the states of higher l vanish at $\mathbf{r}=0$.

In sp impurities, which possess no intrinsic magnetic moment, the magnetization is transferred by the neighbouring magnetic atoms. This has almost no effect on the contribution to $H_{\rm hf}$ from s bound states of the ionic core, but affects the contribution from the valence states strongly. This is found in our calculations, in agreement with previous results [2]; in fact, the valence contribution to $H_{\rm hf}$ is proportional to the local s moment [2, 9]. Thus we focus on the behaviour of the valence s states.

Our starting point is the interpretation of the trends of $H_{\rm hf}$ as a function of the impurity atomic number Z, as it has been understood generally for defects in the bulk of ferromagnetic hosts in the past [2, 14]. Relevant results are shown in figure 1 (bottom right) together with experimental data taken from [1]. The central issue is the so-called s–d *hybridization* of the impurity s orbitals with the d states of the magnetic host, forming bonding (lower in energy) and antibonding (higher) hybrid states. In this way the s local density of states (LDOS) of the impurity is affected, differently for every spin due to the exchange splitting of the host d band. We denote the host majority spin as spin up and the minority as spin down. At the beginning of the series (Ag) the bonding hybrids for both spins are occupied while the antibonding ones are unoccupied. Because the host spin-down d band is higher in energy than the spin-up one, the spin-down bonding hybrids are more s-like than the spin-up ones. Then the impurity s moment is negative and so is $H_{\rm hf}$. As we change Z to the next impurities, the antibonding hybrids come to lower energies and are progressively populated. The first to cross the Fermi level $E_{\rm F}$ is the spin-up antibonding hybrid; thus the s moment and $H_{\rm hf}$ increase and change sign, peaking at iodine. Then the spin-down antibonding hybrid is gradually populated, the s moment decreases again, and so does $H_{\rm hf}$.

Next we turn to cases of reduced coordination. Several coordinations can be realized with the impurity at (001), (111), and (110) surfaces as shown in table 1. The results for $H_{\rm hf}(Z)$ for these coordination numbers N are shown in figure 1. We see that, as the coordination is gradually reduced, the single-peaked structure of $H_{\rm hf}(Z)$ evolves to a double-peaked one. For $N=8$ a 'shoulder' already appears at Sb, and for $N=5$, 4, and 3 there are clearly two maxima of $H_{\rm hf}$ with a local minimum of almost vanishing $H_{\rm hf}$ in between, at Te. A second observation is that, at the beginning of the series, $H_{\rm hf}$ changes sign to positive much earlier at the surface that in the bulk—for $N=4$ and 3 the change has occurred already between Ag and Cd, while in the bulk it occurs at Sn.

To interpret the results we note that the reduced coordination has three effects: firstly the reduction in the transferred magnetic moment, secondly the reduction in the strength of the s–d hybridization, and thirdly the reduction of symmetry. As regards the first effect, a smaller impurity moment does not necessarily lead to a reduced s moment and weaker $H_{\rm hf}$. Indeed, when the second effect is also considered, a weaker s–d hybridization leads to a smaller bonding–antibonding splitting of the s–d hybrids. The antibonding hybrids (in particular for spin up) appear lower in energy for smaller N, and are populated earlier in the sp series, and

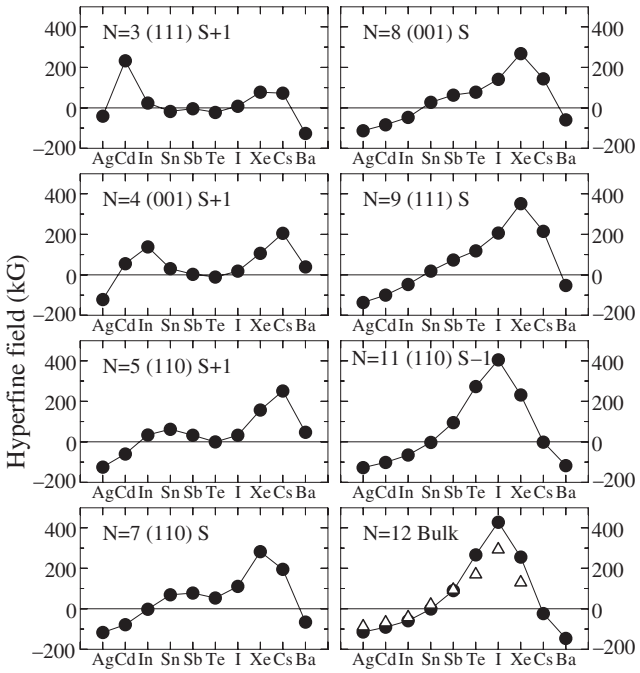

Figure 1. The magnetic hyperfine field of 5sp impurities in Ni bulk and on various Ni surfaces as a function of the impurity atomic number Z. The coordination number N depends on the surface and position (see table 1). As N increases from 3 to 12, the double-peaked structure of $H_{\rm hf}(Z)$ transforms progressively to a single-peaked one. This is related to the gradual decoupling of the s from the p states as explained in the text. For $N = 12$ the triangles show the experimental values [1].

also $H_{\rm hf}$ increases earlier. This is consistent with the rise of $H_{\rm hf}$ for Ag and Cd impurities with reducing coordination.

But there is still the important third effect, i.e., the reduction of symmetry, which results in an interaction of the s with the p states that coexist around $E_{\rm F}$ for sp atoms. In the bulk the impurity has a cubic environment, and the s and p orbitals transform according to different irreducible representations; i.e., an eigenfunction cannot contain orbitals of both kinds simultaneously. As the coordination number is reduced at the surface, cubic symmetry no longer holds, and the s and p orbitals are no longer decoupled. In the cases studied here, if we choose the z axis to be normal to the surface, it is actually the p_z orbital that is coupled with the s (but in a more asymmetric case, such as at a step, all p orbitals would couple). Then s–p hybrids must exist, here in the form $|s\rangle \pm |p_z\rangle$. The s LDOS becomes more complicated, and in particular each of the s–d hybrids discussed above is expected to split into two (one for each s–p hybrid). Although the s–p hybridization should happen even for $N = 11$, it is stronger for smaller coordination numbers when the environment becomes less bulklike.

The new picture is as follows. With reduced coordination, two antibonding s–d hybrids exist per spin, one for each s–p hybrid. At the beginning of the sp series (Ag) only bonding hybrids are occupied and $H_{\rm hf}$ is negative, similarly to the bulk case. In the next elements the first antibonding hybrid (which is more s-like since the p states are still high) crosses $E_{\rm F}$, first for spin up, leading to an increase of $H_{\rm hf}$, and then for spin down, leading to a decrease. Thus the first peak of $H_{\rm hf}$ is formed (for $N = 7$, 5, 4, and 3, at Sb, Sn, In, and Cd, respectively).

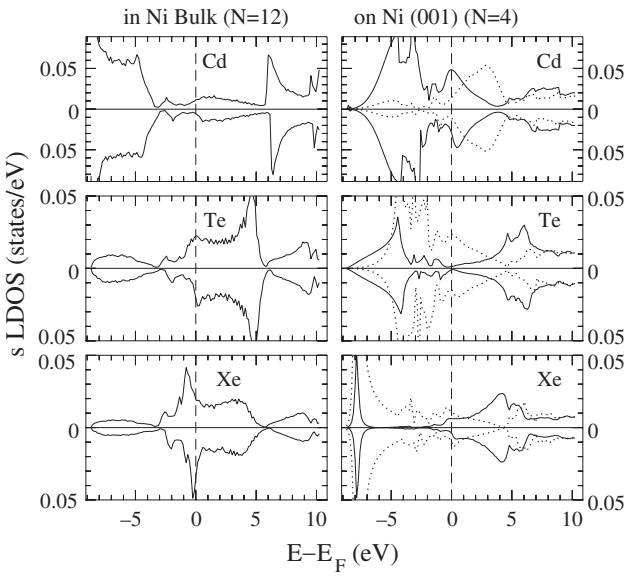

Figure 2. The spin-resolved s LDOS of Cd, Te, and Xe impurities in bulk Ni (left) and on Ni (001) (right, full curves). For the adatoms, the p_z LDOS is also shown by dotted curves; for Te and Xe the p_z LDOS has been scaled by a factor of 0.5. Note also the different scale for Cd compared to Te and Xe. Upper panels correspond to spin up, lower panels to spin down.

As N is reduced the first peak moves toward the beginning of the series because the s–d hybridization is weaker and the first s–d antibonding states are lower in energy. Afterwards the second antibonding hybrid (now more p-like, since the p states are lower) crosses E_F and becomes populated, again first for spin up (increasing H_{hf}) and then for spin down (decreasing H_{hf}); the second peak in H_{hf} is thus formed. In this way the reduction in symmetry for smaller coordination results in a double-peak structure in H_{hf}. The cases for $N = 8$ and 9 are intermediate—in which the s–p hybridization is weak and the first peak merges with the second one, creating the shoulder at Sb.

In figure 2 the s LDOS is shown for Cd, Xe, and Te impurities in bulk Ni ($N = 12$) and on top of the (001) Ni surface as adatoms ($N = 4$). In the adatom case also the p_z LDOS is presented as dotted curves. First we discuss the progressive filling of the states for impurities in bulk. For Cd, the bonding s–d hybrids are occupied for both spins, and the spin-up antibonding hybrid is just starting to pass through E_F; H_{hf} starts to increase. For Te, the antibonding hybrids are more occupied, and for Xe the spin-down antibonding peak becomes occupied. Thus we have the single-peaked structure of $H_{hf}(Z)$. Now we turn to the adatom case. The s LDOS (full curve) looks different. For Cd, the first antibonding hybrid is at E_F, and is more pronounced than in the bulk due to the reduced coordination and hybridization. The p_z states (dotted curve) are energetically a little higher, but we can already recognize some correlation between s and p at the peaks at -1 eV. H_{hf} is approaching its first maximum. Next, for Te, the first antibonding s hybrid is populated for both spins, while the second is above E_F; a 'neck' of almost zero s LDOS is at E_F, and the s moment and H_{hf} are almost zero. The p states are lower, and an s–p_z correlation is seen as the peaks coincide between -5 eV and E_F. Finally, for Xe, the first antibonding hybrid is low (at -8 eV accompanied by a peak in p_z), while the second is passing by E_F, first for spin up giving the second rise to H_{hf}. The physical situation is not unlike the one presented in [6] for 4sp impurities on Ni(001).

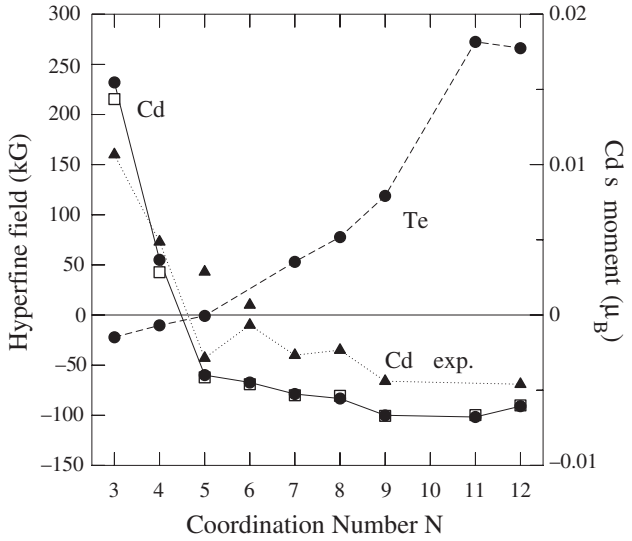

Figure 3. The calculated coordination number dependence of H_{hf} of Cd (full line, full circles) and Te (dashed line) probe atoms on Ni surfaces. The triangles correspond to experimental values reported in [8]. The coordination number N depends on the surface and on the position as described in table 1. While for Cd H_{hf} increases for lower N as the spin-up antibonding s–d hybrids come lower in energy, the situation is opposite for Te, where the on-site s–p hybridization for low N splits the s–d hybrids into two, one populated and one unpopulated, for each spin. The squares show the Cd impurity s moment (right axis), demonstrating its proportionality to H_{hf}.

Now the observed coordination dependence of H_{hf} for Cd probe atoms can be understood. In figure 3, $H_{hf}(N)$ is shown, together with the experimental results [8] and the calculated results for Te probes. For Cd, H_{hf} increases and changes sign for lower N as the spin-up antibonding s–d hybrids come lower in energy, because of the weaker s–d hybridization. The calculated trends agree with the measured data. For $N = 5$ and 6 the positive values are reported in [8], but we make the remark that the sign has not been measured but rather deduced from comparison to calculations for 4sp impurities; thus here we show the same values but also with different sign, according to our calculations. The Cd s moment is also shown, to demonstrate its proportionality to H_{hf}. The trends are opposite for Te, where the on-site s–p hybridization for lower N splits the s–d hybrids into two, one populated and one unpopulated, for each spin. This means that the parabolic decrease of $H_{hf}(N)$ measured for Cd is not necessarily present for other impurities. Rather, each impurity has its own characteristic trend, seen also in the data of figure 1, depending on the position of the hybrids. As regards the proportionality between the H_{hf} and the s moment, we find the ratio of H_{hf} to the s moment to be about 15 000 kG/μ_B for the early 5sp impurities (up to Sn), independent of the coordination, and about 50 000 kG/μ_B for the late 5sp impurities; the reason for the change, as explained in [9], is the change in the form of the valence 5s wavefunction, as an additional node moves into the atomic region.

We now discuss the limitations of the calculations. The local density approximation has been known to underestimate the core electron contribution to H_{hf} in transition elements in the middle of the 3d (Mn and Fe) and 4d series (Ru and Rh) [2, 13], but otherwise it gives reasonable agreement with experiment for impurities in bulk. The terms other than the Fermi contact interaction that are neglected in the present work include the dipole and orbital moment terms. They can contribute to H_{hf} in the absence of cubic symmetry, and can be of the order

of a few per cent compared to the contact term for sp impurities at Fe/Ag interfaces [5]; for Ni they should be smaller due to the smaller magnetic moment. Finally, atom relaxations, which are not included here, are known to affect $H_{\rm hf}$ for impurities in bulk Fe by a few per cent, by changing the strength of the s–d hybridization and shifting the antibonding states in the LDOS [15]; they should have a similar effect in Ni.

4. Conclusions

In conclusion, using first-principles calculations we have interpreted the measured [8] coordination dependence of $H_{\rm hf}$ in Cd impurities in Ni. Our results show a strong, nonlinear dependence on the coordination number N, in agreement with experiment. We have also predicted that the dependence of $H_{\rm hf}(N)$ of the other 5sp impurities in Ni is not decreasing as in Cd; rather, each impurity exhibits its own 'fingerprint' behaviour. The reduced coordination gradually lowers the antibonding s–d hybrids in energy, and more importantly reduces the symmetry, causing an on-site s–p hybridization. Thus the trends of $H_{\rm hf}$ for reduced coordination are different to the ones in the bulk. The effects should be similar for sp impurities of the other lines of the periodic table, and also for other ferromagnetic hosts. We hope that our results will stimulate future experiments.

Acknowledgments

The author is grateful to Professor P H Dederichs and Dr H H Bertschat for useful discussions. Financial support from the Research and Training Network 'Computational Magnetoelectronics' (contract RTN1-1999-00145) of the European Commission is gratefully acknowledged.

Note added in proof. The author was recently informed of a work in progress on similar *ab-initio* calculations of hyperfine fields and electric field gradients, including atomic relaxations (S Cottenier, V Bellini, M Cakmak, F Manghi and M Rots, manuscript in preparation) (Stefaan.Cottenier@fys.kuleuven.ac.be).

References

[1] Rao G N 1985 *Hyperfine Interact.* **24–26** 1119
Mohsen M and Pleiter F 1988 *Hyperfine Interact.* **39** 123
[2] Akai H, Akai M, Blügel S, Drittler B, Ebert H, Terakura K, Zeller R and Dederichs P H 1990 *Prog. Theor. Phys. Suppl.* **101** 11
[3] Granzer H, Bertschat H H, Haas H, Zeitz W-D, Lohmüller J and Schatz G 1996 *Phys. Rev. Lett.* **77** 4261
Bertschat H H, Granzer H, Haas H, Kowallik R, Seeger S and Zeitz W-D 1997 *Phys. Rev. Lett.* **78** 342
Runge B U, Dippel M, Filleböck G, Jacobs K, Kohl U and Schatz G 1997 *Phys. Rev. Lett.* **79** 3054
Swinnen B, Meersschaut J, Dekoster J, Langouche G, Cottenier S, Demuynck S and Rots M 1997 *Phys. Rev. Lett.* **78** 362
Swinnen B, Meersschaut J, Dekoster J, Langouche G, Cottenier S, Demuynck S and Rots M 1998 *Phys. Rev. Lett.* **80** 1569
Bertschat H H, Blaschek H-H, Granzer H, Potzger K, Seeger S, Zeitz W-D, Niehus H, Burchard A, Forkel-Wirth D and the ISOLDE Collaboration 1998 *Phys. Rev. Lett.* **80** 2721
Bertschat H H 1999 *J. Magn. Magn. Mater.* **198/199** 636
Bertschat H H, Granzer H, Potzger K, Seeger S, Weber A, Zeitz W-D and Forkel-Wirth D 2000 *Hyperfine Interact.* **129** 475
[4] Bellini V, Zeller R and Dederichs P H 2001 *Phys. Rev.* B **64** 144427
[5] Rodriguez C O, Ganduglia-Pirovano M V, Peltzer y Blanca E L and Petersen M 2001 *Phys. Rev.* B **64** 144419
Mazet T, Tobola J, Venturini G and Malaman B 2002 *Phys. Rev.* B **65** 104406
[6] Mavropoulos Ph, Stefanou N, Nonas B, Zeller R and Dederichs P H 1998 *Phys. Rev. Lett.* **81** 1505

[7] Pleiter F and Hohenemser C 1982 *Phys. Rev.* B **25** 106
Voigt J, Fink R, Krausch G, Luckscheiter B, Platzer R, Wöhrmann U, Ding X L and Schatz G 1990 *Phys. Rev. Lett.* **64** 2202
[8] Potzger K, Weber A, Bertschat H H, Zeitz W-D and Dietrich M 2002 *Phys. Rev. Lett.* **88** 247201
[9] Mavropoulos Ph, Stefanou N, Nonas B, Zeller R and Dederichs P H 1998 *Phil. Mag.* **78** 435
[10] Papanikolaou N, Zeller R and Dederichs P H 2002 *J. Phys.: Condens. Matter* **14** 2799
[11] Stefanou N, Akai H and Zeller R 1990 *Comput. Phys. Commun.* **60** 231
Stefanou N and Zeller R 1991 *J. Phys.: Condens. Matter* **3** 7599
[12] Koelling D D and Harmon B N 1977 *J. Phys. C: Solid State Phys.* **10** 3107
[13] Blügel S, Akai H, Zeller R and Dederichs P H 1987 *Phys. Rev.* B **35** 3271
[14] Kanamori J, Katayama-Yoshida H and Terakura K 1981 *Hyperfine Interact.* **8** 573
Kanamori J, Katayama-Yoshida H and Terakura K 1981 *Hyperfine Interact.* **9** 363
Akai M, Akai H and Kanamori J 1985 *J. Phys. Soc. Japan* **54** 4246
Akai M, Akai H and Kanamori J 1985 *J. Phys. Soc. Japan* **54** 4257
Akai M, Akai H and Kanamori J 1987 *J. Phys. Soc. Japan* **56** 1064
[15] Korhonen T, Settels A, Papanikolaou N, Zeller R, Dederichs P H, Cottenier S and Haas H 2000 *Phys. Rev.* B **62** 461